Journal of Electronic Materials, Vol. 20, No. 6, 1991

Layer Intermixing and Related Long-Term Instability in Heavily Carbon-Doped AlGaAs/GaAs Superlattices

I. SZAFRANEK, M. SZAFRANEK, J. S. MAJOR, JR.,[a] B. T. CUNNINGHAM,[b] L. J. GUIDO,[c] N. HOLONYAK, JR. and G. E. STILLMAN

Center for Compound Semiconductor Microelectronics, Materials Research Laboratory Coordinated Science Laboratory, University of Illinois at Urbana-Champaign, IL 61801

Superlattices (SLs) of $Al_{0.3}Ga_{0.7}As$/GaAs grown by metalorganic chemical vapor deposition and heavily doped with carbon using $CClp_4$ were annealed for 24 h at 825° C under a variety of ambient and surface encapsulation conditions. Photoluminescence at $T = 1.7$ K has been employed to determine approximate Al-Ga interdiffusion coefficients ($D_{Al\text{-}Ga}$) for different annealing conditions. For all encapsulants studied $D_{Al\text{-}Ga}$ increases with increasing As_4 pressure in the annealing ampoule. This result disagrees with trends reported for Mg-doped crystals, and with predictions of the charged point-defect (Fermi-level) model. The Si_3N_4 cap provides the most effecitve surface sealing against ambient-stimulated layer interdiffusion ($D_{Al\text{-}Ga} \approx 1.5\text{–}3.9 \times 10^{-19}$ cm^2/sec). The most extensive layer intermixing has occurred for an uncapped SL annealed under As-rich ambient ($D_{Al\text{-}Ga} \approx 3.3 \times 10^{-18}$ cm^2/sec). These values are up to ~40 times greater than those previously reported for nominally undoped AlGaAs/GaAs SLs, implying that the C_{As} doping slightly enhances layer intermixing, but significantly less than predicted by the Fermi-level effect. The discrepancies between the experimental data and the model are discussed. Pronounced changes in the optical properties of the annealed SLs with storage time at room temperature are also reported. These changes may indicate a degraded thermal stability of the annealed crystals due to high-temperature-induced lattice defects. A possibly related effect of the systematic failure to fabricate buried heterostructure quantum well lasers via impurity-induced layer disordering in similarly doped AlGaAs/GaAs crystals is discussed.

Key Words: AlGaAs/GaAs, superlattice, layer interdiffusion, carbon doping.

I. INTRODUCTION

The dependence of Al-Ga interdiffusion in quantum well heterostructures (QWHs) and superlattices (SLs) on anneal ambient and surface encapsulation conditions has been extensively investigated under both intrinsic and impurity-induced regimes for $Al_xGa_{1-x}As$/GaAs and related III/V material systems (for a recent review, see Ref. 1). Based on results of that work a consistent picture has evolved, whereby the self-diffusion of Group III host atoms, which causes the layer intermixing, is presumably mediated by the Group III vacancy (V_{III}) and interstitial (I_{III}) charged native point defects.[1–5] The concentrations of these defects depend on the Fermi level position and crystal stoichiometry, and can be experimentally controlled by doping and/or the anneal ambient atmosphere.[1–5] Specifically, Al-Ga interdiffusion has been found to increase in n-type SL crystals with heavy doping of either Group IV (*e.g.*, Si)[4] or Group VI (*e.g.*, Se)[6] substitutional donors during anneals under As-rich ambient, both conditions enhancing solubility of the negatively charged V_{III}. On the other hand, when a SL is *p*-type with a heavy doping of Group II-on Ga sublattice elements (*e.g.*, Mg),[4] increased interface smearing has been observed after Ga-rich anneals, supposedly because of an excess concentration of positively charged I_{III} defects.[1–5]

Recent advances in heavy carbon doping of GaAs and $Al_xGa_{1-x}As$ grown by metalorganic chemical vapor deposition (MOCVD)[7,8] have allowed, for the first time, tests of the trends outlined above also for this Group IV-on-As sublattice acceptor species.[9] In that work[9] the extent of Al-Ga interdiffusion was found to be extremely small compared to other *p*-type dopants, and could not be detected with conventional microanalytical techniques such as cross-sectional two-beam transmission electron microscopy (TEM) or secondary-ion mass spectrometry (SIMS). This led to the conclusion that heavy C_{As} doping suppresses layer disordering in $Al_xGa_{1-x}As$/GaAs SLs relative to an undoped crystal. Also, using low-resolution photoluminescence (PL) at $T = 77$ K, lack of interdiffusion enhancement under Ga-rich compared to As-rich annealing conditions was observed.[9] These recent results obviously disagree with previous data on impurity-induced layer disordering (IILD) in general, and the Fermi-level (or charged point-defect) interdiffusion model,[2–5] in particular.

a) Intel Doctoral Fellow.

b) Now at Raytheon Research, 131 Spring Street, Lexington, MA 02173.

c) Now at Yale University, Department of Electrical Engineering, Center for Micro-electronic Materials and Structures, Box 2157 Yale Station, New Haven, CT 06520.

(Received August 14, 1990; revised November 26, 1990)

0361-5235/1991/1401-409$5.00©91 TMS

Because of the central importance of the data on IILD in heavily C-doped SL crystals to the understanding of the Group III self-diffusion, we have performed a more complete, quantitative study of anneal ambient and surface encapsulation effects on this process. In the present work low-temperature, weak-excitation PL has been employed for improved spectral resolution. The layer disordering-induced shifts to higher energies (ΔE) of the $n = 1$ electron-to-heavy hole ($e \rightarrow hh$) confined-particle transitions were analyzed to yield Al-Ga interdiffusion coefficients ($D_{\text{Al-Ga}}$) for different annealing conditions at $T = 825°$ C. The present work confirms one of the major conclusions of the earlier study.[9] We have observed clear trends of enhanced interface smearing in SLs annealed under As-rich relative to As-deficient ambients for all cases of crystal surface sealing. However, the calculated values of $D_{\text{Al-Ga}}(825°\text{ C})$ fall in the range of $\sim 1.5 \times 10^{-19} - 3.3 \times 10^{-18}$ cm^2/sec, which is higher than the previously reported $D_{\text{Al-Ga}} \approx 8 - 10 \times 10^{-20}$ cm^2/sec for undoped SLs.[3] This indicates a slight enhancement of the interdiffusion process in the C-doped crystals relative to intrinsic conditions (for a compilation of the latter data see Ref. 3). Thus, although a weak IILD effect is operative in heavily C-doped p-type $Al_{0.3}Ga_{0.7}As/GaAs$ SLs in agreement (at least qualitative) with the Fermi-level model,[2-5] a revision is required with regard to the identity of the native defects that may be responsible for the Group III self-diffusion in the presence of large concentrations of substitutional acceptor impurities on the As sublattice.

The layer intermixing effect is promoted by native defects whose concentrations increase at elevated temperatures. An important aspect of the potential applicability of the high-temperature heat treatments is the influence that such processes may have on the long-term stability of the optical and electrical properties of the annealed crystals. In this paper we present an evidence of significant changes in luminescence properties of $Al_xGa_{1-x}As/GaAs$ SL crystals doped with C using CCl_4 source, during storage of several months at room temperature following annealing at 825° C. This effect possibly indicates a structural instability of the annealed crystals due to high-temperature-induced lattice defects and, therefore, it may bear on performance of laser diodes and other electrooptical devices realized using IILD processing. Specifically, a systematic failure to fabricate buried heterostructure QW lasers using IILD in similarly doped crystals is reported.

II. EXPERIMENTAL PROCEDURE

The SL crystal investigated here was grown by low-pressure MOCVD in an EMCORE GS3100 reactor on a 2° off (100) oriented liquid-encapsulated Czochralski GaAs substrate. Trimethylgallium (TMGa), trimethylaluminum (TMAl) and 100% arsine (AsH_3) were the growth precursors, and the carbon doping soure was a 500 ppm mixture of CCl_4 (Matheson) in high-purity H_2.[7] The flow rates of CCl_4 $\approx$ 100 sccm and $H_2 \approx 9$ slm resulted in an approximately uniform carbon doping level of [C] $\approx 8 \times 10^{18}$ cm^{-3} throughout the whole epitaxial multilayer stack of GaAs and $Al_xGa_{1-x}As$, as confirmed by SIMS concentration depth profiles. The growth was carried out at $T \approx 620°$ C, pressure $p \approx 100$ Torr, growth rate $\approx$ 500Å/min, V/III ratio $\approx$ 160 and substrate rotation rate $\approx$ 1500 rpm. The SL crystal consists of a ~700Å thick GaAs buffered layer, followed by 40 $Al_{0.3}Ga_{0.7}As/GaAs$ periods of equal barrier and well thicknesses $L_B \approx L_Z \approx$ 200Å. The SL is confined with a ~200Å $Al_{0.8}Ga_{0.2}As$ layer and further capped with a ~200Å GaAs layer.

The anneals were performed in evacuated quartz ampoules (volume ≈ 3 cm^3, $p \approx 10^{-6}$ Torr) at $T = 825°$ C for 24 hours. Three sets of samples were annealed in separate ampoules under different conditions of the crystal surface stoichiometry: (i) As-rich ambient, (+As), achieved by adding 25 mg of elemental As resulting in an As_4 overpressure of about 2.5 atm in the sealed ampoule at 825° C; (ii) Ga-rich conditions, (+Ga), maintained by placing an elemental Ga in the ampoule to create a very As-deficient ambient corresponding to the equlibrium between the As_4 vapor from the SL crystal and the excess Ga at $T = 825°$ C; and (iii) equilibrium GaAs conditions, (+0), existing when neither As nor Ga is added to the ampoule, so that the more volatile As atoms evaporate from the crystals until equilibrium is reached between the vapor and the Ga-rich epitaxial crystal surface. A set of three samples was loaded into each ampoule. Two SL crystals were encapsulated with an ~1000Å thick layer of either SiO_2 or Si_3N_4 deposited by CVD at ~400 and ~700° C, respectively, and the third sample had an uncapped surface.

The carrier concentration depth profile in the as-grown SL was measured with Polaron PN4200 capacitance-voltage electrochemical profiler. The as-grown and some annealed samples were analyzed also with TEM and SIMS. As asserted earlier, these techniques did not provide much useful information concerning the layer intermixing process. The TEM data confirmed the precalibrated thicknesses $L_B \approx L_Z \approx$ 200Å in the as-grown SL crystal.

The optical properties of all the samples were assessed with low-temperature PL. The samples were mounted strain-free in superfluid ^{4}He at $T \approx 1.7$ K, and were illuminated with the 5145Å line from an Ar^+ laser using low-level excitation of ~36 mW/cm^2. An unfocused beam of about 3 mm in diameter was used to probe almost the entire area of the samples, thus averaging over possible lateral inhomogeneities of the crystals. The emitted radiation was dispersed by an Instruments SA 1m double spectrometer and detected by a thermoelectrically cooled GaAs photomultiplier tube, using the photon counting technique.

III. DATA ANALYSIS

The dominant feature in the low-temperature PL spectrum of the as-grown SL crystal shown in Fig.

1 (dashed curve) is a single, broad peak (full-width at half maximum FWHM ≈ 17.6 mV) at ~1.531_6 eV. This peak is attributed to $n = 1$ electron-to-heavy hole ($e \rightarrow hh$) confined-particle recombination in GaAs quantum wells. The observed emission energy matches within 0.1 meV the value for a square-wave potential in a multiple QWH, calculated using the algorithm of Kolbas and Holonyak[10] with boundary conditions modified to satisfy continuity of $(1/m^*)d\Psi/dz$, in order to account for different effective masses across the well/barrier heterointerfaces.[11,12] The parameters used in the calculations are: $L_B = L_Z = 200$Å, x_Z(Al) = 0, x_B(Al) = 0.3, $m_e^* = 0.0665 + 0.0835x$,[13,14] $m_{hh}^* = 0.34 + 0.42x$,[13,14] $E_g(x) = E_g$ (GaAs) + $1.247x$,[15] E_g (GaAs) = 1.5192 eV at $T = 1.7$ K,[16] and the conduction band-edge discontinuity $\Delta E_c = 0.6\Delta E_g^{\Gamma}$.[13,17] The deviation of ~0.1 meV in the calculated transition energy corresponds roughly to a 1% error in m^* or to a fraction of a monolayer (<2Å) uncertainty in L_Z. Since the actual uncertainties in values of all the parameters are much greater than that (*e.g.*, at least ±10Å for L_Z and L_B), the fit accuracy of ~1 meV is sufficient for our purposes.

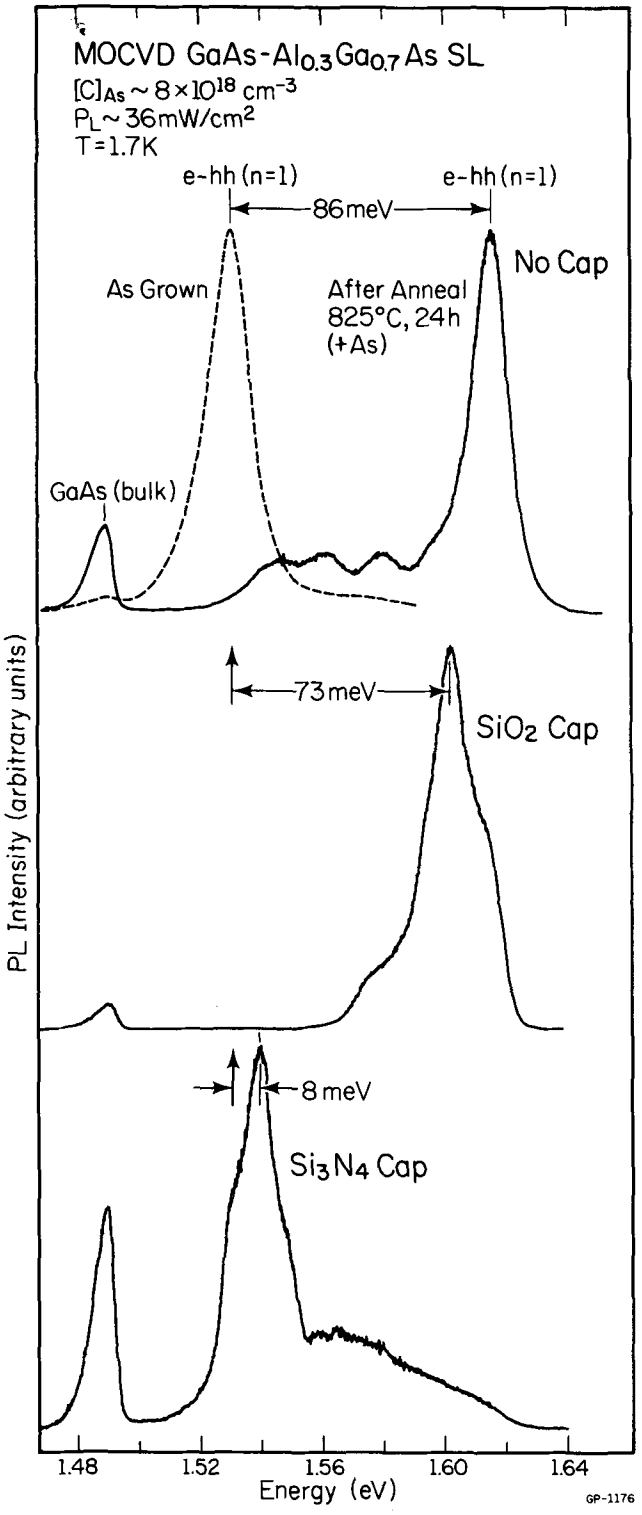

Fig. 1 — Photoluminescence spectra of the as-grown (dashed line) and annealed heavily C-doped $Al_{0.3}Ga_{0.7}As$/GaAs superlattice crystals. The effect of surface encapsulation on Al-Ga interdiffusion efficiency under As-rich annealing ambient is demonstrated by variations in the energy shift of the $(e \rightarrow hh)_{n=1}$ emission relative to the as-grown sample. A stable low-energy peak at ~1.49 eV due to bulk GaAs is also shown.

For $L_Z = 200$Å, the binding energies of both free and neutral acceptor-bound heavy-hole excitons are ~7 meV.[18] If the main SL peak observed experimentally (Fig. 1) were due to annihilation of these excitons, this would imply an $(e \rightarrow hh)_{n=1}$ energy between ~7 to ~14 meV higher than the calculated value. However, it should be pointed out that the specified barrier and well dimensions are the lower limits of these quantities, as determined from growth calibration, TEM and SIMS. Furthermore, the TEM image of the as-grown SL shows abrupt interfaces. Finally, computer simulations indicate that correction to the calculated $(e \rightarrow hh)_{n=1}$ photon energy due to inaccuracy in x_B (or ΔE_g) should be at most of the order of ~1 meV. It is, therefore, impossible to account for an underestimate as large as ~7–14 meV, and we conclude that despite the low temperature of 1.7 K, formation of free excitons and their subsequent capture at C acceptors are suppressed in these SL crystals, presumably due to delocalization effects caused by the high doping level.[19] It follows, that the SL-related transition observable in PL spectrum of the as-grown sample originates most probably in the $(e \rightarrow hh)_{n=1}$ recombination process, as asserted at the beginning of this section.

The PL spectra of the annealed SLs also exhibit a single prominent transition at $h\nu > E_g$(GaAs), accompanied by usually weak shoulders and secondary peaks on both high and low-energy sides (Fig. 1). The important assumption underlying our analysis is that the dominant SL peaks in the PL spectra of the as-grown and annealed crystals are of the same origin. With this assumption, we can deduce the Al-Ga interdiffusion coefficients from the measured shifts to higher energies, ΔE, of the emission lines in the annealed SLs relative to the as-grown one, as discussed later. The additional, weaker spectral features seen in Fig. 1 may result from depth-dependent extent of layer intermixing,[20] giving rise to a wide range of confined-particle bound states detected with PL.

The large depth penetration of the PL probe is manifested directly by the presence of a broad band

at ~1.49 eV, also shown in Fig. 1. This transition comes from unresolved conduction band-to-acceptor (e–A^0) and donor-to-acceptor (D^0–A^0) recombination processes due to C acceptors in the bulk GaAs, namely the cap and buffer layers as well as the substrate. The latter assignment has been supported by the PL spectra measured from the back surface of the substrate. The observation of occasionally very intense GaAs luminescence through the ~1 μm thick SL stack indicates a large ambipolar diffusion length of the photo-generated carriers and/or a photon recycling effect.[21] The peak position of this transition is invariant with annealing conditions, thus confirming that it is not related to the SL structure, and providing an intrinsic calibration of the extent of Al-Ga interdiffusion in each case of annealing conditions. Moreover, changes in the relative intensity of this peak may serve as a sensitive monitor of varying transport properties of the annealed SL crystals, as we discuss in Sec. 4.3.

The energy shift ΔE due to layer disordering-induced modification of the SL compositon profile after annealing under given conditions allows an approximate determination of the corresponding Al-Ga interdiffusion coefficient, $D_{\text{Al-Ga}}$.[22–24] The confined-particle energy levels in finite potential wells of the conduction and heavy-hole valence bands are calculated by solving the one-dimensional, time-independent Schrödinger equation with the appropriate Hamiltonian:[11,12]

$$\left[-\frac{h^2}{2}\frac{\partial}{\partial z}\frac{1}{m^*(z)}\frac{\partial}{\partial z} + V(z) \right] \Psi(z) = E\Psi(z). \quad (1)$$

Considering only the lowest ($n = 1$) bound states in each band, a symmetric envelope wave function[24]

$$\Psi(z) = \sum_{k=0}^{\infty} c_k \cos\left(\frac{2\pi kz}{T}\right) \quad (2)$$

is used, where $T = L_Z + L_B$ is the period of the superlattice. The periodic potential profile is determined by the interdiffusion-modified alloy composition profile. We have solved Fick's equation with constant $D_{\text{Al-Ga}}$ using Fourier series expansion[25] to satisfy the initial conditions of the periodic square-well potential profile, and the boundary condition:

$$x_\infty \equiv x(z, t \to \infty) = (L_B x_B + L_Z x_Z)/T \quad (3)$$

where x_B and x_Z are the Al mole fractions in the barriers and wells, respectively. The general solution for the SL composition profile is:

$$x(z,t) = x_\infty + \frac{2}{\pi}(x_z - x_B)\sum_{k=1}^{\infty} \cdot\left\{\frac{1}{k}\sin\left(\frac{\pi kL_z}{T}\right)\left(\frac{2\pi kz}{T}\right)\exp\left[-\left(\frac{2\pi k}{T}\right)^2 Dt\right]\right\}. \quad (4)$$

For a given annealing time t,

$$V_{c,v}(z) = PF_{c,v}\,[x(z,t) - x(0,t)], \quad (5)$$

where F_c and F_v are the conduction and valence band offsets, and P is the proportionality constant of Vegard's law ($P = 1.247$ for $Al_xGa_{1-x}As$ with $x \leq 0.45$[15]). Substitution of Eqs. 2 and 5 in Eq. 1, followed by the standard orthogonalization procedure of multiplying both sides of the Schrödinger equation by $\cos(2\pi lz/T)$, where l is an integer ($0 \leq l \leq k_{\max}$), and integrating over one period gives the characteristic matrix of the eigenvalue problem:

$$[A + B]\,c = Ec, \quad (6)$$

where A and B are the matrices resulting from the orthogonalization procedure on the kinetic and potential energy operators, respectively. Integration by parts yields a simplifed form of the matrix A:

$$A_{k,l} = 2\left(\frac{h}{T}\right)^2 kl \cdot\int_0^{T/2}\frac{1}{m^*(z)}\sin\left(\frac{2\pi kz}{T}\right)\sin\left(\frac{2\pi lz}{T}\right)dz, \quad (7)$$

which for a general $m^*(z) = f(x)$ is computed numerically. The elements of the matrix B can be calculated analytically:

$$B_{k,l} = \begin{cases} B_\infty & k = l = 0 \\ B_\infty + Q(2k) & k = l > 0 \\ Q(l) & k = 0,\ l > 0 \\ Q(k+l) + Q(k-l) & k \neq l,\ k > 0 \end{cases} \quad (8)$$

where

$$B_{00} = PF_{c,v}\,[x_\infty - x(0,t)] \quad (9)$$

and

$$Q(n) = \frac{PF_{c,v}}{\pi n}(x_Z - x_B) \cdot\sin\left(\frac{\pi nL_z}{T}\right)\exp\left[-\left(\frac{2\pi n}{T}\right)^2 Dt\right], \quad (10)$$

with the integer parameter n defined for each matrix element as shown in Eq. 8.

The number of Fourier components ($k_{\max} + 1$) included in the calculations is increased until the convergence criterion of the relative change of <0.1% in an energy of the $n = 1$ bound state is met, which corresponds to ~10 μeV for the SL structure discussed in this paper. For an almost square-well potential profile more than 30 Fourier series terms may be necessary for the eigenvalues to converge, while about 10 terms are typically sufficient for graded bands. For each measured value of ΔE a conjugate

gradient iterative procedure was applied to find $D_{Al\text{-}Ga}$ such that $|\Delta E_{exp} - \Delta E_{calc}| < 0.1$ meV. An example of the potential profiles for the as-grown and two annealed SL structures shown in Fig. 1, as well as the corresponding $n = 1$ confined-particle bound states and $(e \rightarrow hh)_{n=1}$ transitions are presented schematically in Fig. 2.

This method is very sensitive to the SL structural parameters. For example, an uncertainty of about one monolayer in $L_Z \approx 200$Å causes up to 10% change in $D_{Al\text{-}Ga}$ in the low-diffusivity regime of $\sim 10^{-19}$ cm^2/sec. However, the high accuracy (~0.2 meV) in the PL data is sufficient to draw unambiguous conclusions with regard to the influence of the surface encapsulation and annealing ambient on the extent of AlGaAs/GaAs heterointerface disordering.

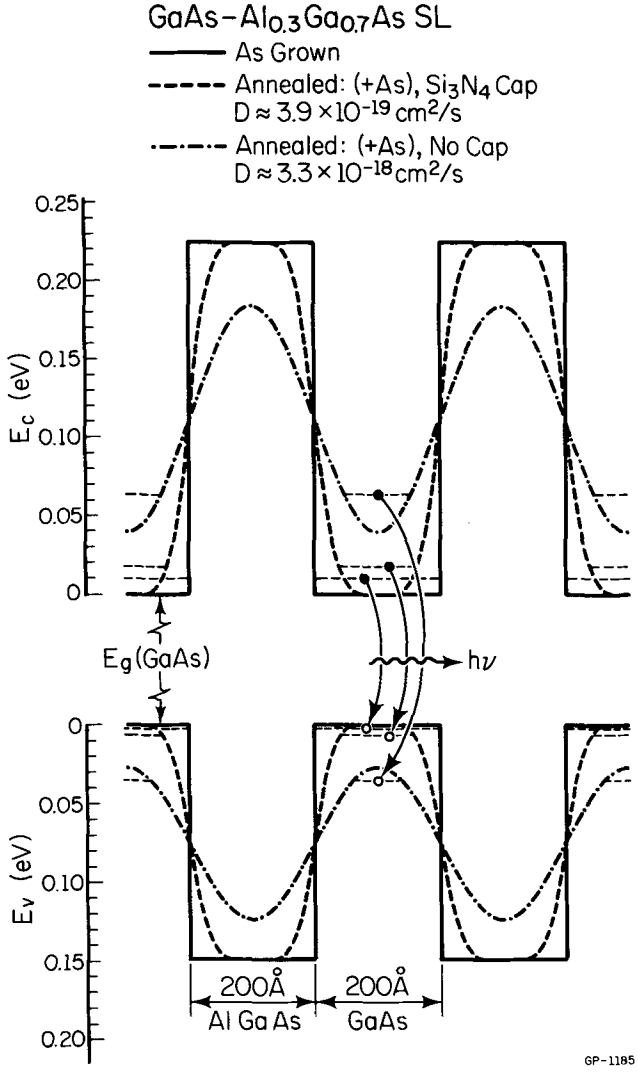

Fig. 2 — Potential energy profiles of $Al_{0.3}Ga_{0.7}As/GaAs$ SL before (square-wave, solid line) and after 24 hr long anneal under (+As) ambient with Si_3N_4 cap (dashed curve) and with no cap (chained line), based on the data presented in Fig. 1 and Table I. The horizontal dashed lines show the confined-particle bound states calculated for each potential profile. Also indicated are the $(e \rightarrow hh)_{n=1}$ transitions corresponding to the measured photoluminescence.

IV. RESULTS

4.1: *Surface Encapsulation Effects*

Photoluminescence measurements examining the effects of encapsulation on the extent of interface smearing in the SLs capped with 1000Å thick SiO_2 and Si_3N_4 films relative to the unprotected sample are shown in Fig. 1 for the (+As) anneal ambient. As discussed in the following section, the As-rich atmosphere significantly enhances the interdiffusion in the C-doped crystals, and hence it offers the most sensitive conditions for evaluation of the influence of the encapsulation on retarding the SL disordering. Equivalent trends were observed also for the other two annealing ambients studied, however.

The most extensive SL composition profile grading leading to the greatest PL energy shift observed in this work, $\Delta E \approx 86$ meV, occurred for the capless sample, as shown in the top spectrum of Fig. 1. The SiO_2 cap is permeable to Ga and, thus, provides a very ineffective surface encapsulation relative to the uncapped crystal.[26–28] This effect of Ga out-diffusion-induced layer intermixing can be seen in Fig. 1, where $\Delta E \approx 73$ meV for SiO_2 cap is the second largest SL peak energy shift measured in our study.

As expected, the most efficient encapsulation against Al-Ga interdiffusion stimulated by crystal interaction with the ambient atmosphere was provided by the Si_3N_4 cap.[26,28] The most extensive interface grading after 24 hr anneal with this encapsulant was observed again for the (+As) ambient, but it resulted in a PL energy shift only of ~8 meV, as shown in the bottom spectrum of Fig. 1. Our data indicate that the Si_3N_4 layer, although relatively nonporous, does not entirely block in and out-diffusion of Al, Ga and As, since a clear dependence of ΔE on the annealing ambient has been observed for the Si_3N_4 cap as well, as summarized in Table I.

4.2: *Anneal Ambient Effects*

Regardless of crystal encapsulation, an obvious monotonic trend of decreasing extent of layer inter-

Table I. Peak Energy Up-shifts of the $(e \rightarrow hh)_{n=1}$ Transitions in Annealed C-doped $Al_{0.3}Ga_{0.7}As/GaAs$ SL Crystals Relative to the As-grown Sample, and the Corresponding Al-Ga Interdiffusion Coefficients at $T = 825°$ C, for Different Encapsulation and Ambient Conditions.

Cap		Annealing Ambient (+Ga)	(+0)	(+As)
None	ΔE [meV]	27–38	N/A	86
	D [cm^2/sec]	$1.1–1.5 \times 10^{-18}$	—	3.3×10^{-18}
SiO_2	ΔE [meV]	31	59	73
	D [cm^2/sec]	1.3×10^{-18}	2.2×10^{-18}	2.8×10^{-18}
Si_3N_4	ΔE [meV]	3.1	6.7	8.0
	D [cm^2/sec]	1.5×10^{-19}	3.3×10^{-19}	3.9×10^{-19}

mixing on transition from As-rich to As-deficient (or Ga-rich) annealing conditions is evident in our data. This is demonstrated in Fig. 3 for SiO_2-capped, and in Fig. 4 for capless SL crystals. In both cases significant variations in the PL energy shifts relative to the as-grown sample can be noticed as a function of the anneal ambient. As mentioned above, a similar behavior has been observed also for the Si_3N_4-capped samples, but in this case over a much narrower spectral range of $\sim 3 \leq \Delta E \leq \sim 8$ meV. The spectroscopic data and the corresponding calculated $D_{Al\text{-}Ga}$ are summarized in Table I.

4.3: Instability of Annealed Superlattice Crystals

The PL spectra shown in Figs. 1, 3 and 4, as well as those used for compilation of the data in Table I were measured a few weeks after the SL crystals had been grown and annealed. All the samples were then repeatedly measured under identical experimental conditions several times during a period of about one year, while being stored at room temperature. Practically no changes have been observed in either the position or the line shape of the $(e \rightarrow hh)_{n=1}$ peak as a function of storage time for the as-grown crystal, compared to the initial spectrum shown at the top of Fig. 1 (dashed curve). In contrast, virtually all samples that underwent the post-growth high-temperature treatments have exhibited clearly discernable variations in their PL spectra. The extent of these spectral modifications and their nature vary from sample to sample, and no prevailing trend for increased Al-Ga interdiffusion with time could be identified.

Three representative examples of the instability effect, covering various encapsulation and annealing ambient conditions, are shown in Figs. 5–7. Figure 5 presents two PL spectra measured at different times after the Si_3N_4-capped SL was annealed at (+As) atmosphere. In this case, after a few months of storage at room temperature the $(e \rightarrow hh)_{n=1}$ peak position shifted up from 1.539_6 to 1.542_7 eV and the total line width increased from 20.1 to 24.5 meV. In additional PL measurements taken on this sample, both the position and the line width of this peak have continued to fluctuate. Stability of the bulk GaAs peak at ~1.488 eV during storage of the annealed samples at room temperature not only confirms the precision of the instrumental calibration in the different PL measurements, but also indicates that the spectral modifications are limited to the AlGaAs/GaAs multilayer stack. This fact suggests that the instability of the optical properties is related to long-term structural changes taking place in the annealed SL crystals, presumably due to high-temperature-induced lattice defects.

Another example of SL instability is shown in Fig. 6 for the SiO_2-capped sample annealed under (+0) conditions. In this case the line shape changes of the SL-related luminescence are less pronounced, and the main effect is a significant energy up-shift of the dominant SL peak from 1.590_5 to 1.596_7 eV

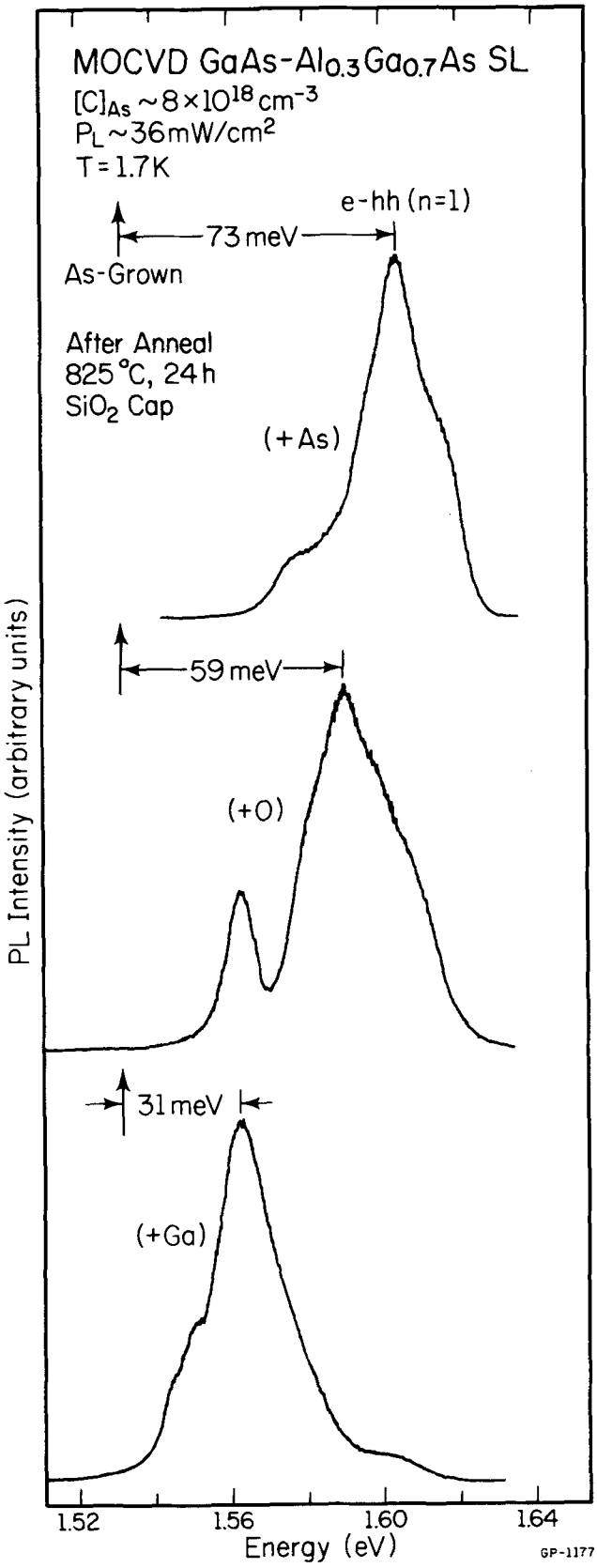

Fig. 3 — Photoluminescence spectra of heavily C-doped $Al_{0.3}Ga_{0.7}As/GaAs$ superlattice crystals annealed with SiO_2 cap under (+As), (+0) and (+Ga) ambients. A monotonic trend of enhanced layer disordering with increasing As_4 pressure in the ampoule is evident by comparing the energy shifts of the dominant SL luminescence from each annealed sample relative to that of the as-grown sample.

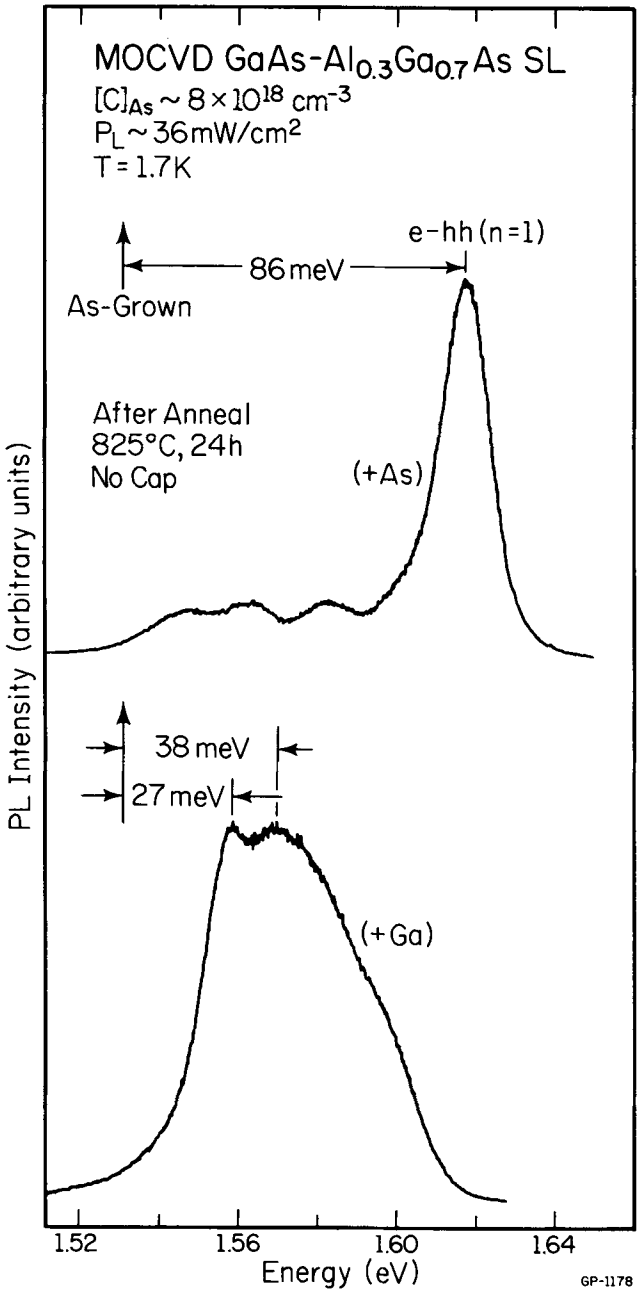

Fig. 4 — Photoluminescence spectra of heavily C-doped $Al_{0.3}Ga_{0.7}As/GaAs$ superlattice crystals annealed with uncapped surface under (+As) and (+Ga) ambients. A clear trend of enhanced layer disordering with increasing As_4 pressure in the ampoule is evident by comparing the energy shifts of the dominant SL luminescence from each annealed sample relative to that of the as-grown sample.

with respect to the stable emission line of the bulk GaAs at ~1.488 eV. As in Fig. 5, the relative PL intensity of the latter peak increased slightly with storage time. Similar changes, occasionally much more dramatic and leading to approximately equal PL intensities from the bulk GaAs and the QWs, have been observed for almost all of the annealed samples, alongside modifications of the Sl-related luminescence. The varying intensity of this deep emission may be indicative of changing carrier transport properties of the annealed SLs with stor-

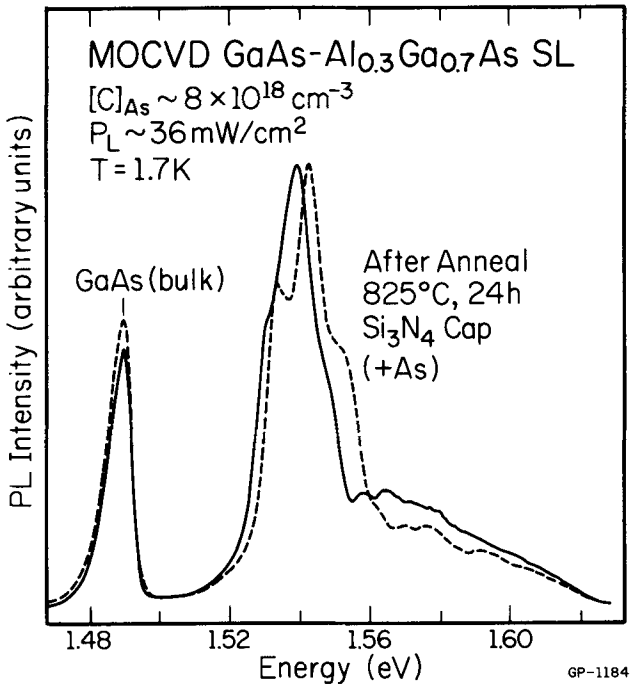

Fig. 5 — Photoluminescence spectra of an annealed, heavily C-doped $Al_{0.3}Ga_{0.7}As/GaAs$ superlattice crystal, demonstrating the effect of instability of its optical properties as a function of storage time at room temperature. The solid-line spectrum was measured shortly after the sample was grown and annealed, and the dashed-line spectrum after several months of storage at room temperature.

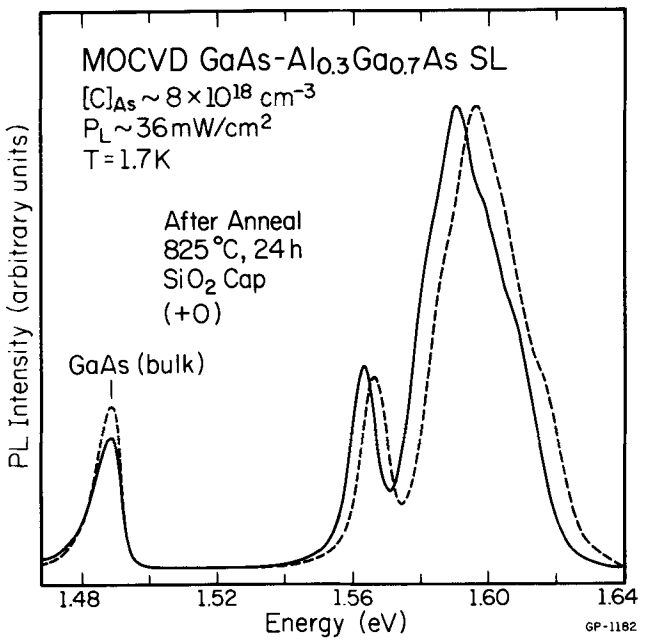

Fig. 6 — Same as Fig. 1, but for different encapsulation and ambient conditions. A pronounced energy up-shift of the SL-related luminescence after a few months of room-temperature storage is evident, compared to a stable peak position of the bulk GaAs emission at ~1.488 eV. Variation in the relative PL intensity of the latter peak possibly indicates changes in electrical transport properties of the annealed SL crystals during storage at room temperature.

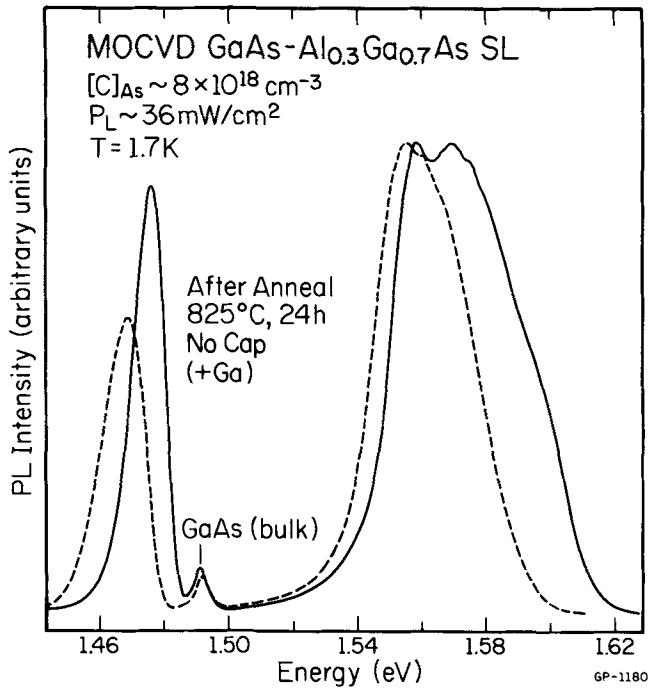

Fig. 7 — Same as Figs. 1 and 2, but for different surface encapsulation and annealing ambient conditions. The shift to lower energy of the $(e \rightarrow hh)_{n=1}$ transition in the dashed spectrum precludes a continuing process of layer disordering during storage at room temperature as a possible explanation of the instability effect.

age time at room temperature, providing additional support for the SL instability argument.

The room-temperature instability of the capless SL annealed under (+Ga) ambient is shown in Fig. 7. After a few months of storage the SL-related luminescence transformed from a broad doublet at 1.559_0–1.569_3 eV (the solid-line spectrum) into a narrower single peak at 1.555_4 eV (the dashed curve in Fig. 7). Such a down-shift in PL energy rules out an ongoing process of post-anneal interface disordering as a possible interpretation of the PL changes with time. In this sample and a few others, an intense PL peak on the low-energy side of the bulk GaAs band has been detected. For the SL in Fig. 7 this peak has shifted from 1.475_8 to 1.468_6 eV and the FWHM increased from 11.9 meV to 15.5 meV. We stop short at speculating on the exact origin of the recombination process giving rise to this peak, but the facts that the PL energy and line shape become significantly modified, as opposed to the stable bulk GaAs line at ~1.49 eV, seem to imply that this transition is SL-related. With increasing sample temperature in the 1.7–21 K range this peak quenches rapidly, while both shifting and broadening toward lower energy, opposite of the behavior expected from $(e$–$A^0)$ and $(D^0$–$A^0)$ recombination processes in bulk material.

Within the limited data available, the most stable annealed SL structures have been those that underwent the most extensive layer intermixing during the thermal treatments, namely the capless and SiO_2-capped crystals annealed under (+As) ambient. In both cases there was practically no line shape modification and the $(e \rightarrow hh)_{n=1}$ peak position shifted by less than 2 meV. This result may suggest that the latent potential for further structural changes after annealing is relatively reduced when significant Al, Ga and native defect self-diffusion takes place during the high-temperature processing.

Anomalous behavior has also been observed in Si-IILD buried heterostructure laser diodes fabricated from $Al_xGa_{1-x}As/GaAs$ and $Al_yGa_{1-y}As/GaAs/In_xGa_{1-x}As$ QWH laser material employing C (from CCl_4) as the p-type dopant. Figure 8 shows the curves of threshold current density (J_{th}, A/cm^2) versus reciprocal length (1/L, cm^{-1}) for broad area diodes fabricated from both as-grown (Fig. 8-a) and annealed (Fig. 8-b) C-doped (CCl_4) QWH laser diode material. The anneal procedure employed here is 12 hr at 825° C under As overpressure. For the anneal cycle the sample is encapsulated with CVD Si_3N_4. After the anneal the calculated distributed gain and loss parameters, β and α, respectively, have both decreased slightly, although the overall performance of the QWH laser diode material following the anneal cycle is still quite acceptable. The parameters β and α have been calculated using[29]

$$J_{th} = \alpha/\beta - [\ln(R_1R_2)]/(2\beta L), \qquad (11)$$

where L is the laser diode bar length and R_1 and R_2 are the mirror reflectances. Since these anneal conditions are similar to those used in the fabrication of index-guided laser diodes via Si-IIILD, C-doped (CCl_4) QWH laser diode structures should be excellent candidates for Si-IILD procedures. However, to date we have been unable to fabricate Si-IILD diodes from a large variety of either $Al_xGa_{1-x}As/GaAs$ or strained-layer $Al_yGa_{1-y}As/GaAs/In_xGa_{1-x}As$

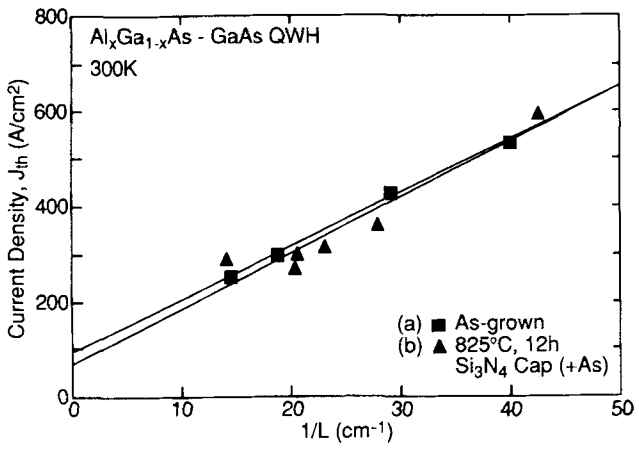

Fig. 8 — Threshold current density (J_{th}, A/cm^2) versus reciprocal length (1/L, cm^{-1}) for broad area diodes fabricated from both as-grown (a) and annealed (b) C-doped (CCl_4) QWH laser diode material. The gain parameter, β, has values of 0.090 and 0.085 cm/A for as-grown and annealed C-doped QWH material, respectively. The distributed loss parameter, α, has also decreased during the anneal from an as grown value of 8.33 cm^{-1} to an annealed value of 5.53 cm^{-1}. Following the anneal, the general lasing characteristics of the material remain acceptable.

QWH laser crystals employing C from CCl_4 as the *p*-type dopant. Although these data are as yet unexplained, it should be noted that Si-IILD laser diodes operating cw at 300 K up to a current of $I = 7I_{th}$, where $I_{th} \approx 25$ mA is the average threshold current, have been fabricated from structures grown in the same Emcore GS3100 reactor used in this work, employing C from TMGa as the *p*-type dopant.[30]

V. DISCUSSION

The PL data and the corresponding Al-Ga interdiffusion coefficients for the whole matrix of the C-doped SL crystals annealed under different ambient conditions with various surface encapsulants, are summarized in Table I. Using a similar approach, Schlesinger and Kuech[23] and Lee *et al.*,[24] determined $D_{Al\text{-}Ga} \approx 9.7 \times 10^{-20}$ cm^2/sec for a nominally undoped $Al_{0.3}Ga_{0.7}As/GaAs$ quantum well system annealed with Si_3N_4 cap at 825° C. Tan and Gösele[3] compiled the available data on Ga self-diffusion and Al-Ga interdiffusion under intrinsic conditions and obtained $D_{Al\text{-}Ga}(825°\text{ C}) \approx 8.4 \times 10^{-20}$ cm^2/sec. Our results range from $D_{Al\text{-}Ga} = 1.5\text{–}3.9 \times 10^{-19}$ cm^2/sec for Si_3N_4 caps to $D_{Al\text{-}Ga} = 1.1\text{–}3.3 \times 10^{-18}$ cm^2/sec for the samples with uncapped surfaces, over the whole investigated range of As_4 pressure in the ampoules. These diffusivity values are higher than those for undoped crystals, indicating an effect of slight impurity-induced layer disordering enhancement in C-doped *p*-type AlGaAs/GaAs SLs. We believe that the present quantitative conclusion is more reliable than that recently published,[9] which was based on a qualitative evaluation of TEM images. From simulations of a SL composition profile as a function of Al-Ga interdiffusion we have noticed that for typical SL structures used in our IILD studies (*e.g.*, Refs. 4, 9 and the present work), the transition from a high TEM alloy contrast to a practically irresolvable image may take place over a less than one order of magnitude range of $D_{Al\text{-}Ga}$.

The relatively weak interdiffusion enhancement measured in our work is quantitatively consistent with earlier results for Be-doped and implanted SLs,[31–33] as discussed by Tan and Gösele,[2,3] as well as with our estimate of the lower bound of $D_{Al\text{-}Ga} \approx 5 \times 10^{-17}$ cm^2/sec in Mg-doped crystal reported by Deppe *et al.*[4] In all these cases the observed IILD effect is significantly less extensive than the $D_{Al\text{-}Ga} \propto (p/n_i)^{\alpha}$ dependence predicted by the Fermi-level model,[2,3,5] where $\alpha = +2$ is the charge state of the Group III interstitials.[34] The measured values of $D_{Al\text{-}Ga}$ set an upper limit of $\alpha = 1$, thus clearly disagreeing with the charged point-defect model.[2–5]

Furthermore, Ralston *et al.*[33] reported a significant difference between the effect of implanted Be vs. Mg on layer intermixing. Similarly, Deppe *et al.*[4] demonstrated a complete destruction of a Mg-doped SL structure after a 10 hr anneal at 815° C under (+0) ambient which, as mentioned above, corresponds to a lower bound of $D_{Al\text{-}Ga} \approx 5 \times 10^{-17}$ cm^2/sec. This value is more than one order of magnitude greater than the highest $D_{Al\text{-}Ga}$ value determined in this work for the C-doped crystals (Table I). These discrepancies indicate dopant species dependence of IILD in *p*-type SLs. In particular, they suggest that a negligible enhancement of Al-Ga interdiffusion in C and some Be-doped *p*-type crystals with grown-in (as opposed to diffused-in) dopants is probably not a general effect, and as such it lacks a proper explanation by the Fermi-level model.

The dependence of the interdiffusion efficiency on annealing ambient in heavily C-doped SLs reported in this paper raises additional questions with regard to the charged-defect model in its present form.[1–5] The model implies that the doping level and type, by determining the Fermi-level position,[2,3] and the annealing atmosphere, by affecting the crystal stoichiometry,[1,4,5] are the dominant factors controlling the concentration of the charged defects which are believed to assist in Group III self-diffusion, namely Group III vacancies (V_{III}) and interstitials (I_{III}). The model predicts that because of the electronic energy contribution to the total free energy of a semiconductor, the layer disordering in *p*-type materials proceeds via the interstitialcy mechanism involving positively charged, donorlike I_{III}. A strong enhancement of the interdiffusion in Mg-doped SLs annealed under Ga-rich relative to As-rich surface conditions,[4] has seemed to directly support such notion. However, the unambiguous trend of increasing layer intermixing with increasing As_4 pressure [$p(As_4)$] in the annealing ambient, that we have observed for heavily C-doped *p*-type SLs with all analyzed forms of surface encapsulation, obviously contradicts the $D_{Al\text{-}Ga} \propto [1/p(As_4)]^{1/4}$ dependence predicted by the Fermi-level model.[5]

A plausible explanation for the observed IILD enhancement under As-rich conditions is that other point defects, and in particular As interstitial I_{As} and As antisite defect As_{III} become active in Al-Ga interdiffusion mechanism in the presence of Group IV majority substitutional impurities on the As sublattice. For example, annihilation of I_{As} on a Group III sublattice can generate I_{III} and As_{III} via the kick-out process:

$$I_{As} \leftrightarrow As_{III} + I_{III}, \tag{12}$$

thus bringing about an excess non-equilibrium concentration of I_{III} defects even under (+As) anneal ambient. Since all the point-defects in Eq. 12 are donor-like,[34] their solubility is expected to be relatively high in *p*-type crystals. Moreover, Coulomb interaction between the positively charged As_{III} and I_{III}, as well as a Group III concentration gradient due to the very As-rich surface which acts as a I_{III} sink boundary, would then enhance I_{III} out-diffusion and, consequently, layer disordering. Naturally, because of very low absolute concentrations of the defects in Eq. 12, this process is not expected to be as effective as may be the case for a highly soluble and diffusive Group II impurity such as Zn. The latter species, which can be present in relatively large concentrations in crystal while occupying both sub-

stitutional and interstitial sites, participate directly in diffusion of Group III sublattice host and dopant atoms through the interstitialcy mechanism.[2,3,5]

VI. CONCLUSIONS

The first quantitative data on impurity-induced layer intermixing of AlGaAs/GaAs SLs in heavily C-doped crystals have been reported for different surface encapsulation and annealing ambient conditions. As expected, the Si_3N_4 cap provided the best surface encapsulation and reduced the extent of IILD by about one order of magnitude compared to both uncapped and SiO_2-capped crystals. A slight enhancement of $D_{Al\text{-}Ga}$ for [C] $\approx 8 \times 10^{18}$ cm^{-3} has been observed relative to previously published results for nominally undoped SL structures.[3] However, the extent of layer intermixing is quantitatively inconsistent with the Fermi-level model,[2-5] which significantly overestimates the $D_{Al\text{-}Ga}$ values.

For all surface encapsulation conditions studied, a monotonic trend of increasing $D_{Al\text{-}Ga}$ with increasing $p(As_4)$ in an ampoule has been observed. This behavior is opposite to that predicted by the charged point-defect model[2-5] and, therefore, it suggests that the model in its present form, where the Al-Ga interdiffusion in p-type crystals is assumed to be mediated mainly by Group III interstitials, lacks general validity.

A two-fold species dependence of IILD has been discussed: (i) a significant difference in the absolute magnitude of $D_{Al\text{-}Ga}$ in Mg vs C-doped SLs for nominally the same concentrations of these two acceptor impurities; and (ii) an opposite dependence of layer intermixing on the annealing ambient in these two cases. The species dependence is not accounted for at all by the Fermi-level-effect model[2-5] in its present form.

Finally, thermodynamic instability of annealed C-doped AlGaAs/GaAs SL crystals is apparent through the pronounced changes in their luminescence properties observed in this study. It is plausible that this effect results from structural modifications of the SL layers due to high-temperature-induced lattice defects and, therefore, it may have important implications on performance of devices based on IILD processing, as demonstrated here for buried heterostructure QW lasers doped with C from CCl_4 source. Since similar AlGaAs/GaAs structures grown at high temperatures (760–825° C) using C doping from TMGa allowed fabrication of high-quality laser diodes via IILD,[30] it is conceivable that the anomalous behavior of the crystals doped with C from CCl_4, grown at lower temperatures, is related to increased O_2 concentrations in AlGaAs layers and/or other growth-induced effects specific to C doping with the CCl_4 source.

ACKNOWLEDGMENTS

The technical assistance of M. K. Suits, R. MacFarlane and R. T. Gladin in preparation of this manuscript is appreciated. This work was supported by the Joint Services Electronics Program, under contract N00015-84-C-0149, by the National Science Foundation, under grants DMR 86-12860 and CDR 89-43166 and by SDIO/IST under contract No. DAAL 03-89-K-0080 administered by the Army Research Office.

REFERENCES

1. D. G. Deppe and N. Holonyak, Jr., J. Appl. Phys. *64*, R93 (1988).
2. T. Y. Tan and U. Gösele, J. Appl. Phys. *61*, 1841 (1987).
3. T. Y. Tan and U. Gösele, Appl. Phys. Lett. *52*, 1240 (1988).
4. D. G. Deppe, N. Holonyak, Jr., W. E. Plano, V. M. Robbins, J. M. Dallesasse K. C. Hsieh and J. E. Baker, J. Appl. Phys. *64*, 1838 (1988).
5. R. M. Cohen, J. Appl. Phys. *67*, 7268 (1990).
6. D. G. Deppe, N. Holonyak, Jr., K. C. Hsieh, P. Gavrilovic, W. Stutius and J. Williams, Appl. Phys. Lett. *51*, 581 (1987).
7. B. T. Cunningham, M. A. Haase, M. J. McCollum and G. E. Stillman, Appl. Phys. Lett. *54*, 1905 (1989).
8. B. T. Cunningham, J. E. Baker and G. E. Stillman, Appl. Phys. Lett. *56*, 836 (1990).
9. L. J. Guido, B. T. Cunningham, D. W. Nam, K. C. Hsieh, W. E. Plano, J. S. Major, Jr., E. J. Vesely A. R. Sugg, N. Holonyak, Jr. and G. E. Stillman, J. Appl. Phys. *67*, 2179 (1990).
10. R. M. Kolbas and N. Holonyak, Jr., Amer. J. Phys. *52*, 431 (1984).
11. W. A. Harrison, Phys. Rev. *123*, 85 (1961).
12. D. J. BenDaniel and C. B. Duke, Phys. Rev. *152*, 683 (1966).
13. R. C. Miller, D. A. Kleinman and A. C. Gossard, Phys. Rev. *B 29*, 7085 (1984).
14. P. Lavaetz, Phys. Rev. *B 4*, 3460 (1971).
15. H. C. Casey, Jr. and M. B. Panish, Heterostructure Lasers: Part A; Fundamental Principles (Academic, Orlando, 1978), p. 192.
16. D. D. Sell, Phys. Rev. *B 6*, 3750 (1972).
17. M. A. Haase, M. A. Emanuel, S. C. Smith, J. J. Coleman and G. E. Stillman, Appl. Phys. Let. *50*, 404 (1987).
18. D. C. Reynolds, K. K. Bajaj, C. W. Litton, P. W. Yu, W. T. Masselink, R. Fischer and H. Morkoc, Phys. Rev. *B 29*, 7038 (1984).
19. P. J. Dean and D. C. Herbert, In *Excitons*, ed. K. Cho (Springer, Berlin, 1979), p. 131.
20. L. J. Guido, N. Holonyak, Jr., K. C. Hsieh and J. E. Baker, Appl. Phys. Lett. *54*, 262 (1989).
21. J. L. Bradshaw, W. J. Choyke, R. P. Devaty and R. L. Messham, J. Appl. Phys. *67*, 1483 (1990).
22. M. D. Camras, N. Holonyak, Jr., R. D. Burnham, W. Streifer, D. R. Scifres, T. L. Pauli and C. Lindström, J. Appl. Phys. *54*, 5637 (1983).
23. T. E. Schlesinger and T. Kuech, Appl. Phys. Lett. *49*, 519 (1986).
24. J.-C. Lee, T. E. Schlesinger and T. F. Kuech, J. Vac. Sci. Technol. *B 5*, 1187 (1987).
25. J. Crank, The Mathematics of Diffusion, 2nd edition (Clarendon/Oxford University, London, 1975), p. 17.
26. K. V. Vaidyanathan, M. J. Helix, D. J. Wolford, B. G. Streetman, R. J. Blattner and C. A. Evans, Jr., J. Electrochem. Soc. *124*, 1781 (1977).
27. D. G. Deppe, L. J. Guido, N. Holonyak, Jr., K. C. Hsieh, R. D. Burnham, R. L. Thornton and T. L. Paoli, Appl. Phys. Lett. *49*, 510 (1986).
28. L. J. Guido, J. S. Major, Jr., J. E. Baker, W. E. Plano, N. Holonyak, Jr. and K. C. Hsieh, J. Appl. Phys. *67*, 6813 (1990).
29. J. I. Pankove, "Optical Processes in Semiconductors" (Dover, New York, 1975), p. 218.
30. L. J. Guido, G. S. Jackson, D. C. Hall, W. E. Plano and N. Holonyak, Jr., Appl. Phys. Lett. *52*, 522 (1988).
31. M. Kawabe, N. Shimizu, F. Hasegawa and Y. Nannichi, Appl. Phys. Lett. *46*, 849 (1985).
32. Y. Hirayama, Y. Suzuki and H. Okamoto, Jpn. J. Appl. Phys. *24*, 1498 (1985).
33. J. Ralston, G. W. Wicks, L. F. Eastman, B. C. De Cooman and C. B. Carter, J. Appl. Phys. *59*, 120 (1986).
34. G. A. Baraff and M. Schlüter, Phys. Rev. Lett. *55*, 1327 (1985).